Journal of Materials Processing Tech. 259 (2018) 341–345

Contents lists available at ScienceDirect

Journal of Materials Processing Tech.

journal homepage: www.elsevier.com/locate/jmatprotec

Anti-fouling of submerged entry nozzle with electric current pulse

Xin Yang, Zhaoyang Liu*, Jingkun Yu*

School of Metallurgy, Northeastern University, Shenyang, 110819, PR China

ARTICLE INFO

Keywords:
Electric current pulse
Submerged entry nozzle
Clogging
Interfacial properties

ABSTRACT

An effective method for anti-clogging of submerged entry nozzle (SEN) was developed by imposing an electric current pulse (ECP) between the SEN and the stopper in the continuous casting process. The morphologies and components of the adhered inclusions on the inner wall of SEN were examined. The size distribution and amounts of inclusions in the steel slab were measured and compared before and after treatment with ECP. After ECP treatment, the tap hole of SEN was only slightly clogged, the inner wall became smooth and the thickness of adhered inclusions decreased by about 50%. The ECP effect was also reflected in the inclusion amounts of the formed steel slab, which decreased by approximately 30% compared to the non-treated sample. These improvements were attributed to the ECP transferring excess negative charges to the molten steel side and maintaining a low or even a zero electric potential difference between the SEN and molten steel, which decreased the wettability and the interaction between the two phases.

1. Introduction

1.1. Background

Submerged entry nozzles (SENs) made of refractory materials are used during the continuous casting process to connect the tundish and the mold, in order to help to protect the molten steel from re-oxidation and splashing (Mertke and Aneziris, 2015). However, the inner wall and the tap hole of SEN are prone to buildup of non-metal inclusions, especially in aluminum-killed steel (Sun et al., 2008a, b) and titanium-containing steel (Basu et al., 2004), which results in the clogging of SEN and severely affects the productivity and quality of steel (Singh, 1974). In order to decrease the clogging of SEN, several measures have been adopted: (1) controlling the amount of deoxidizing agent and reducing the deoxidization products (Yang et al., 2016); (2) calcium treatment to form low melting point compounds (Yang et al., 2013); (3) argon stirring and float acceleration (Lopez et al., 2014); and (4) changing the SEN raw materials and ensuring that the inner wall of SEN is smooth (Vermeulen et al., 2002). These methods can suppress the adhesion of inclusions on the inner wall of SEN to a certain extent. However, it is difficult to completely overcome the SEN clogging problem in the production process.

Several researchers have investigated the unique effects of electric current pulse (ECP) on particles in both aqueous solutions and liquid metal (Liu et al., 2017; Zhang et al., 2014). Zhang and Qin (2015) indicated that the inclusions migrated to the surface of the molten steel under the action of ECP due to the lowering of free energy of system.Zhao and Qin (2017) claimed that the ECP has agglomeration and deformation effects on the inclusions under specific conditions. Sun et al. (2008a,b) used SEN as the electrode material and imposed a 5 A current. They found that the thickness of attachment on the anode was decreased by 90%, while the cathode was increased by 156%. In another study, researchers imposed a direct current of 100 A between the SEN and stopper, and found that the adhesion of alumina on the refractory surface was reduced (Kawamoto, 2011). However, they did not fully explain the mechanism. Moreover, imposing such a large current on SEN is dangerous and resource-wasting in the practical production. Dai et al (2016) reported that a dense inclusion layer was formed on the inner wall of SEN under the action of ECP. However, the mechanism of the anti-clogging effect of electric current on SEN still remains unclear.

1.2. Charging behavior in liquid metal

Paik et al. (1998; 2001; 2004) investigated the surface charging characteristics of different oxides, such as Al_2O_3, SiO_2, Cr_2O_3, NiO, TiO_2 and ZnO, when in contact with molten lead and aluminum. They measured the potential of the compressed diffuse layer and the excess electron density of the flat layer by differential potential analysis and induced electromotive force (EMF) method, respectively. They found that most metal oxides carried positive charges when they came into contact with liquid metal. Recently, Yang et al. (2017) connected the SEN with the ground by using a high precision source meter in the continuous casting process, and found that the SEN was charged when the molten steel flowed through. The electric charges on the SEN side

* Corresponding authors.
E-mail addresses: zhaoyangliu@stumail.neu.edu.cn (Z. Liu), yujk@smm.neu.edu.cn (J. Yu).

https://doi.org/10.1016/j.jmatprotec.2018.05.008
Received 27 October 2017; Received in revised form 30 April 2018; Accepted 2 May 2018
Available online 05 May 2018
0924-0136/

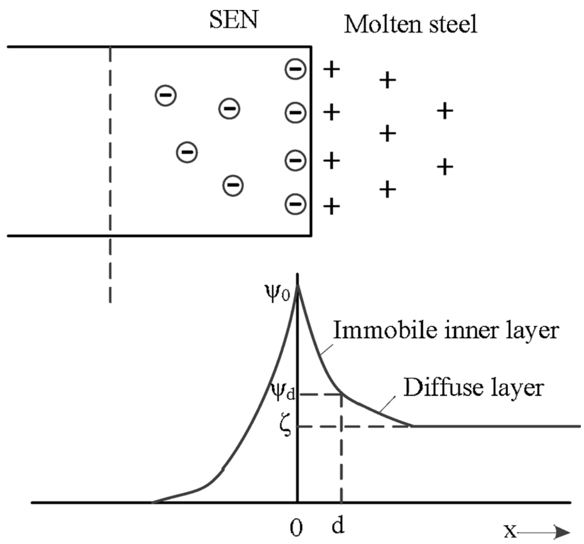

Fig. 1. Potential distribution of the interface between SEN and molten steel.

were negative, and the amount of charges was directly proportional to the steel flow velocity. They explained that the interface between molten steel and inner wall of SEN generated an electric double layer. Equal quantities of opposite charges were present in the steel and SEN sides, respectively. The charges in the molten steel side could be divided into two parts: immobile inner layer and diffuse layer (Fig. 1). When the molten steel flowed through the SEN, the charges in the diffuse layer were carried away, which caused the excess negative charges to be gathered at the SEN side. A potential difference was also generated between the SEN and molten steel (Yu et al., 2017). According to the electro-wetting theory (Mugele and Baret, 2005), the potential difference affects the refractory and molten steel wettability, which accelerates the migration and adhesion of inclusions to the SEN inner wall.

In the present work, an ECP was imposed between SEN and a stopper in the continuous casting process. The microstructure of the adhered inclusions in the inner wall of SEN was investigated. Size distribution and total number of inclusions in the steel slab were measured and compared. A possible mechanism was proposed for the anti-clogging effect of ECP on the SEN.

Table 1
Chemical composition of the low carbon steel (%).

C	Si	Mn	P	S	Al	Als
0.038	0.0101	0.1715	0.0129	0.0084	0.0289	0.0257

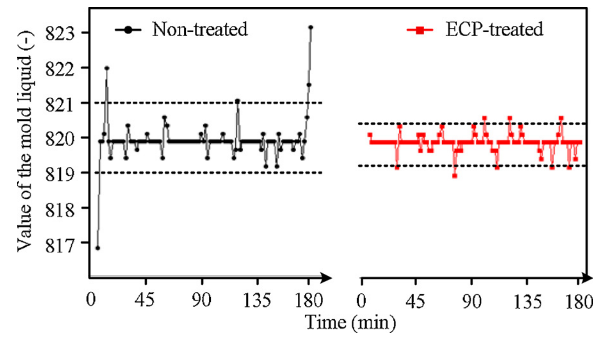

Fig. 3. The mold liquid level in the continuous casting process.

2. Experimental

The experiment was set up in a two-strand continuous casting machine as presented in Fig. 2. The cathode and anode of the electric current pulse generator were respectively connected to the SEN (75 mm inner diameter and 1200 mm length) and stopper using a molybdenum wire, and the connecting position was sealed with high temperature cement to prevent oxidization. The SEN and the tundish were dried at high temperature for 1.5 h, and then the low carbon steel casting was started. A rectangular ECP was imposed between the SEN and the stopper with the current density of 0.1 A/cm^2 and frequency of 20 kHz. The chemical compositions of the low carbon steel are presented in Table 1. At the start of the casting, the same conditions were maintained in the two strands, such as the liquid level, argon flow and stopper position. The molten steel temperature was approximately 1550 °C and the stable casting speed was approximately 1.0 m/s.

After casting, the two SENs were removed and cooled in air. The attachments of the inner wall and tap hole were analyzed by cutting cross-sections of the SEN. The thicknesses of the attachments were measured by a laser range finder with the precision of 1 mm (LRF, PD42, HILTI). The microstructures and chemical compositions of the attachments were investigated through field emission scanning electron microscopy (FE-SEM, Ultra plus, ZEISS) and energy dispersive spectroscopy (EDS), respectively. Moreover, two cubic slab samples of

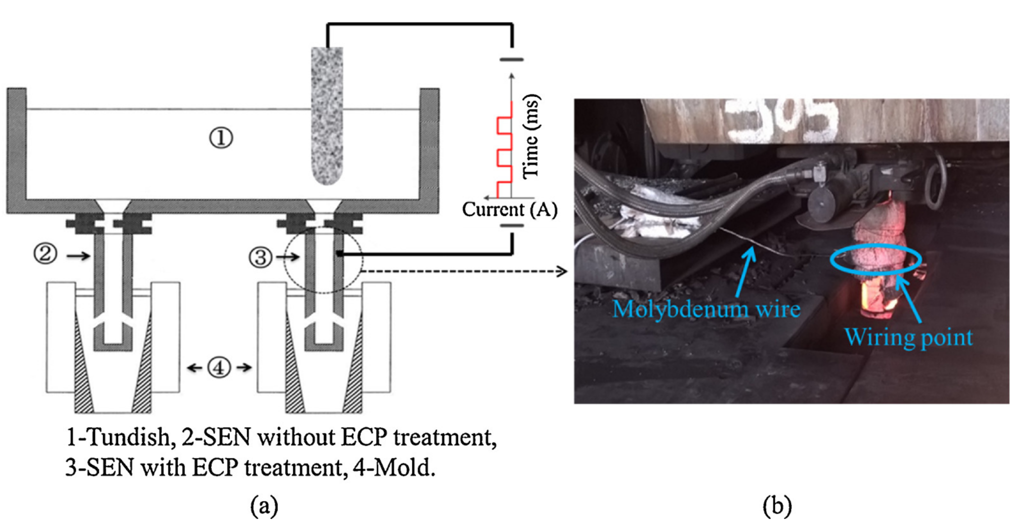

Fig. 2. (a) Schematic diagram of the experimental set up; (b) wiring position.